

Analysis of Indeterminate Contact Forces in Robotic Grasping and Contact Tasks

Yusuke MAEDA, Koutarou ODA and Satoshi MAKITA

Abstract—In this paper, we analyze indeterminate contact forces in robotic grasping and contact tasks. Previous studies by Omata and Nagata showed that there is a constraint on static friction forces, which is derived from contact kinematics, in rigid-body power grasps. The set of possible contact forces can be calculated using the constraint. This approach can be applied to not only mechanical analysis of power grasps but also that of other robotic contact tasks. However, there are some cases where Omata and Nagata's formulation generates paradoxical results on contact forces. In this paper, we investigate this problem and propose a modified method to calculate the set of possible indeterminate contact forces. We also study how to reduce the computation.

I. INTRODUCTION

Mechanics of contact forces plays an important role in various fields such as robotic manipulation, assembly and fixturing. In rigid-body systems, contact forces can be indeterminate especially when there are many contact points. Omata and Nagata analyzed such indeterminate contact forces in rigid-body power grasps in detail and showed that some combinations of static friction forces cannot exist because of their incompatibility with a rigid body motion [1] [2] (Fig. 1). Their idea can be applied not only to mechanical analysis of power grasps but also that of various robotic manipulation [3] [4].

However, in some cases, Omata and Nagata's approach produces paradoxical results on the contact forces (see examples in Section III-B). In this paper, we describe the problem in their approach and propose an improved method to calculate the set of possible indeterminate contact forces in robotic grasping and contact tasks. The key idea was originally presented in our previous papers [3] [4], but they covered only robotic contact tasks such as graspless manipulation [5], and the discussion was limited to specific issues such as evaluation of manipulation robustness and

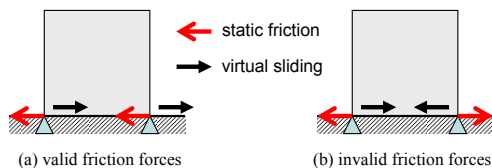


Fig. 1. Valid and invalid friction forces

Y. MAEDA is with Division of Systems Research, Faculty of Engineering, Yokohama National University, 79-5 Tokiwadai, Hodogaya-ku, Yokohama 240-8501 JAPAN, maeda@ynu.ac.jp

K. ODA and S. MAKITA are with Department of Mechanical Engineering, Division of Systems Integration, Graduate School of Engineering, Yokohama National University.

internal force problems. This paper deals with not only contact tasks but also grasping, and gives detailed discussion on how to calculate the set of possible indeterminate forces. Our new method requires combinatorial calculation, so we also study how to reduce the computation.

II. PROBLEM FORMULATION

A. Assumptions and Notation

Let us consider N -fingered grasping. For convenience, we regard all the immobile links, palms and the environment as a part of one virtual finger. Thus, for example, $N = 1$ in the cases as shown in Fig. 1.

In this paper, we make the following assumptions:

- The object, bodies of robot fingers, and the environment are rigid.
- The system is static.
- All the contacts can be approximated by finite number of point contacts.
- Contact normals can be defined at all the contact points.
- Coulomb friction exist at the contact points.
- Each friction cone can be approximated by a polyhedral convex cone [6] with r edge vectors.

The notation used in this paper is as follows:

- M_i : number of contact points on the i -th finger.
- $M := \sum_{i=1}^N M_i$: total number of contact points.
- L_i : number of joints of the i -th finger.
- $L := \sum_{i=1}^N L_i$: total number of joints.
- P_{ij} : the j -th contact point on the i -th finger.
- P_l : the l -th contact point; we put serial number on P_{ij} such that $l = \sum_{n=1}^{i-1} L_n + j$.
- $\mathbf{p}_l \in \mathbb{R}^3$: the position vector of P_l .
- $\mathbf{t}_{l1}, \mathbf{t}_{l2} \in \mathbb{R}^3$: unit tangent vectors at P_l defined such that $\mathbf{t}_{l1}^T \mathbf{t}_{l2} = 0$.
- $\mathbf{c}_{lm} \in \mathbb{R}^3$: the m -th unit edge vector of a polyhedral convex cone that approximates the friction cone at P_l .
- $\mathbf{f}_l \in \mathbb{R}^3$: contact force at P_l .
- $\mathbf{f} := [\mathbf{f}_1^T, \dots, \mathbf{f}_M^T]^T \in \mathbb{R}^{3M}$.
- τ_{ij} : joint torque of the j -th joint of the i -th finger.
- $\boldsymbol{\tau}_i := [\tau_{i1}, \dots, \tau_{iL_i}]^T \in \mathbb{R}^{L_i}$.
- $\boldsymbol{\tau} := [\boldsymbol{\tau}_1^T, \dots, \boldsymbol{\tau}_N^T]^T \in \mathbb{R}^L$.
- θ_{ij} : joint variable of the j -th joint of the i -th finger.
- $\boldsymbol{\theta}_i := [\theta_{i1}, \dots, \theta_{iL_i}]^T \in \mathbb{R}^{L_i}$.
- $\boldsymbol{\theta} := [\boldsymbol{\theta}_1^T, \dots, \boldsymbol{\theta}_N^T]^T \in \mathbb{R}^L$.
- $\mathbf{v}_0 \in \mathbb{R}^3$: virtual translation velocity of the object.
- $\boldsymbol{\omega}_0 \in \mathbb{R}^3$: virtual angular velocity of the object.
- $\mathbf{V} := [\mathbf{v}_0^T, \boldsymbol{\omega}_0^T]^T \in \mathbb{R}^6$.
- $\mathbf{w}_{\text{ext}} \in \mathbb{R}^6$: external wrench applied to the object.

Although the above notation is for spatial cases, we use that with reduced dimensions for planar cases.

B. Mechanical Model

The static equilibrium equation of the object can be written as follows:

$$\mathbf{W}\mathbf{f} = -\mathbf{w}_{\text{ext}}, \quad (1)$$

where

$$\mathbf{W} := \begin{bmatrix} \mathbf{I}_3 & \cdots & \mathbf{I}_3 \\ \mathbf{p}_1 \times \mathbf{I}_3 & \cdots & \mathbf{p}_M \times \mathbf{I}_3 \end{bmatrix} \in \mathbb{R}^{6 \times 3M}; \quad (2)$$

\mathbf{I}_n is the $n \times n$ identity matrix; $\mathbf{p}_l \times \mathbf{I}_3 \in \mathbb{R}^{3 \times 3}$ is a skew-symmetric matrix defined such that $(\mathbf{p}_l \times \mathbf{I}_3)\mathbf{x} \equiv \mathbf{p}_l \times \mathbf{x}$. The relationship between the joint torques and the contact forces are:

$$\mathbf{J}^T \mathbf{f} = \boldsymbol{\tau}, \quad (3)$$

where

$$\mathbf{J} := \text{diag}(\mathbf{J}_1, \dots, \mathbf{J}_N) \in \mathbb{R}^{3M \times L} \quad (4)$$

$$\mathbf{J}_i := \begin{bmatrix} \mathbf{J}_{i1} \\ \vdots \\ \mathbf{J}_{iM_i} \end{bmatrix} \in \mathbb{R}^{3M_i \times L_i}; \quad (5)$$

$\mathbf{J}_{ij} \in \mathbb{R}^{3 \times L_i}$ is the Jacobian matrix between the position of P_{ij} and the joints of the i -th finger.

Equation (1) and (3) can be combined as follows:

$$\mathbf{A}^T \mathbf{f} = \mathbf{w}, \quad (6)$$

where

$$\mathbf{A} := [\mathbf{W}^T \quad \mathbf{J}] \in \mathbb{R}^{3M \times (6+L)} \quad (7)$$

$$\mathbf{w} := [-\mathbf{w}_{\text{ext}}^T, \boldsymbol{\tau}^T]^T \in \mathbb{R}^{6+L} \quad (8)$$

When $\mathbf{w} \in \text{Im}\mathbf{A}^T$, we can obtain the contact forces in the following form by solving (6):

$$\mathbf{f} = \mathbf{h}_0 + \mathbf{h}, \quad \mathbf{h} \in \text{Ker}\mathbf{A}^T, \quad (9)$$

where \mathbf{h}_0 is a particular solution and \mathbf{h} is a homogeneous solution. When $\text{Ker}\mathbf{A}^T \neq \{\mathbf{0}\}$, the contact forces are indeterminate.

The contact forces must also satisfy Coulomb's law. From the assumption of polyhedral convex friction cones, contact force at P_l can be expressed as:

$$\mathbf{f}_l = \mathbf{C}_l \mathbf{k}_l, \quad (10)$$

where

$$\mathbf{C}_l := [\mathbf{c}_{l1} \quad \dots \quad \mathbf{c}_{lr}] \in \mathbb{R}^{3 \times r} \quad (11)$$

$$\mathbf{k}_l := [k_{l1}, \dots, k_{lr}]^T \in \mathbb{R}^r \quad (12)$$

$$k_{lm} \geq 0 \quad (m = 1, \dots, r). \quad (13)$$

Now all the contact forces can be represented as follows:

$$\mathbf{f} = \mathbf{C}\mathbf{k} \quad (\mathbf{k} \geq \mathbf{0}), \quad (14)$$

where

$$\mathbf{C} := \text{diag}(\mathbf{C}_1, \dots, \mathbf{C}_M) \in \mathbb{R}^{3M \times rM} \quad (15)$$

$$\mathbf{k} := [\mathbf{k}_1^T, \dots, \mathbf{k}_M^T]^T \in \mathbb{R}^{rM}. \quad (16)$$

Let us define the following matrices:

$$\mathbf{T}_l := [\mathbf{t}_{l1} \quad \mathbf{t}_{l2}] \in \mathbb{R}^{3 \times 2} \quad (17)$$

$$\mathbf{T} := \text{diag}(\mathbf{T}_1, \dots, \mathbf{T}_M) \in \mathbb{R}^{3M \times 2M}. \quad (18)$$

Then the static friction forces, $\mathbf{f}_t \in \mathbb{R}^{2M}$, can be expressed by:

$$\mathbf{f}_t = \mathbf{T}^T \mathbf{f}. \quad (19)$$

C. Goal of This Paper

Omata and Nagata derived an additional constraint on static friction forces, \mathbf{f}_t , from contact kinematics [1] [2]. However, their method sometimes produces unreasonable results, which are presented in the next section. The goal of this paper is to modify the constraint so that such unreasonable results are excluded. Moreover, we also present a procedure to calculate the set of possible indeterminate contact forces based on the modified constraint.

III. OMATA'S FORMULATION OF CONSTRAINT ON STATIC FRICTION FORCES

A. Virtual Sliding for Deriving Constraint on Friction Forces

Suppose a *virtual* instantaneous motion of the object and the robot fingers that causes *virtual* sliding at some contact points. Note that this virtual sliding is required only to derive the constraint on *static* friction forces and must be distinguished from *actual* sliding, which corresponds to *kinetic* friction forces.

Omata and Nagata claimed that virtual sliding should satisfy the following equation [1] [2]:

$$\mathbf{A} \begin{bmatrix} \mathbf{V} \\ -\boldsymbol{\theta} \end{bmatrix} = \mathbf{T}\dot{\mathbf{Y}}, \quad (20)$$

where

$$\dot{\mathbf{Y}} = [\dot{\mathbf{Y}}_1^T, \dots, \dot{\mathbf{Y}}_M^T]^T \in \mathbb{R}^{2M} \quad (21)$$

$$\dot{\mathbf{Y}}_l = [\dot{Y}_{l1}, \dot{Y}_{l2}]^T \in \mathbb{R}^2; \quad (22)$$

\dot{Y}_{l1} and \dot{Y}_{l2} are the elements of the virtual sliding velocity vector at P_l in the direction of \mathbf{t}_{l1} and \mathbf{t}_{l2} , respectively. The valid virtual sliding must satisfy (20); in other words, $\dot{\mathbf{Y}}$ is valid when there exist \mathbf{V} and $\boldsymbol{\theta}$ that satisfy (20).

Omata and Nagata's idea can be summarized as follows:

- 1) The (virtual) sliding is constrained by contact kinematics, (20).
- 2) Static friction forces act only in the opposite direction of the trend of (virtual) sliding to prevent it.
- 3) Therefore, static friction forces are also constrained.

In the case of Fig. 1, the validity of friction forces can be judged by the above scheme. The virtual slidings as shown in the left of Fig. 1 satisfy (20) and therefore the corresponding static friction forces are valid. On the other hand, the virtual slidings as shown in the right of Fig. 1 do not satisfy (20) and therefore the corresponding static friction forces are invalid.

Omata and Nagata's formulation imposes a "global" constraint on friction forces; in other words, their constraint is on the *combination* of the friction forces. On the other hand, friction models such as Coulomb's law impose only "local" constraints on each of the friction forces.

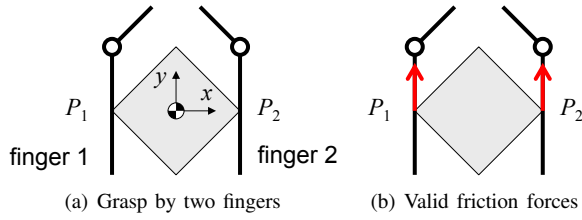


Fig. 2. Example: grasp with two contact points

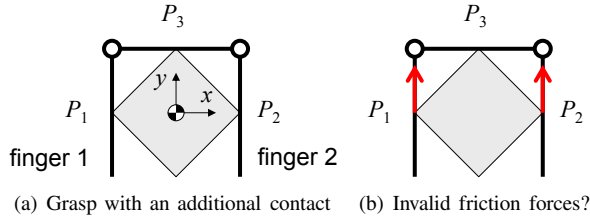


Fig. 3. Example: Grasp with three contact points

B. Paradoxical Results

Let us consider a two-fingered grasp as shown in Fig. 2(a). In this case, when an external force (e.g. gravity) is applied to the object vertically downward, static friction forces shown in Fig. 2(b) can be generated to prevent falling down of the object. Of course, they are valid in Omata and Nagata’s formulation.

Then, let us consider a similar grasp as shown in Fig. 3(a). This grasp has an additional contact between the object and the “palm” (P_3) in comparison to Fig. 2(a). In this case, when an external force is applied to the object vertically downward, static friction forces shown in Fig. 3(b) could also be generated. However, these friction forces are invalid in Omata and Nagata’s formulation; the virtual object motion vertically downward does not satisfy (20), because such a motion will break the contact P_3 .

Intuitively, when a contact point is added to a robotic grasp, the robustness of the grasp should be larger than or equal to the original grasp. However, in Omata and Nagata’s formulation, the additional contact may invalidate some friction forces and make the grasp less robust—this is paradoxical.

Suppose a similar case, as shown in Fig. 4(a). In this case, a rectangular object is just on a plane, not grasped. When an external force is applied downward right to the object, static friction forces shown in Fig. 4(b) can be generated to prevent horizontal sliding of the object. They are valid in Omata and Nagata’s formulation.

Then, let us add a new contact point, P_3 , as shown in Fig. 5(a). In this case, when an external force is applied to the object downward right, static friction forces shown in Fig. 5(b) could also be generated. However, these friction forces are invalid in Omata and Nagata’s formulation; the virtual object motion horizontally to the right does not satisfy (20), because such a motion will break the contact P_3 . This is another paradoxical result.

Note that the occurrence of such paradoxical results is not limited to the above two simple examples.

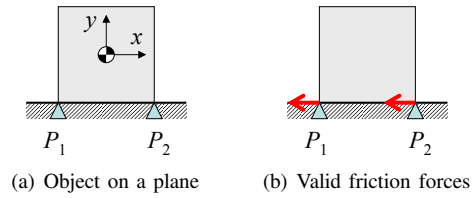


Fig. 4. Example: Non-grasped object with two point contacts

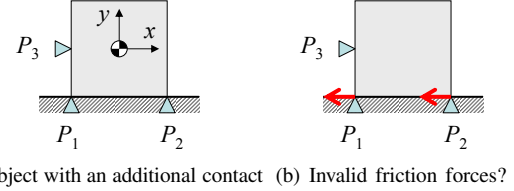


Fig. 5. Example: Non-grasped object on a plane with three contact points

IV. A NEW FORMULATION OF CONSTRAINT ON STATIC FRICTION FORCES

A. Constraint on Virtual Sliding

As shown in the previous section, Omata and Nagata’s formulation sometimes excludes valid contact forces. Why are such results generated? We think that the problem is in (20); this is a constraint on *actual* instantaneous sliding. However, we now consider *virtual* sliding to derive the constraint on static friction forces. Because (20) is too strict for virtual sliding, Omata and Nagata’s formulation sometimes excludes valid virtual slidings and corresponding valid friction forces.

Thus we introduce a new relaxed constraint on virtual sliding instead of (20) as follows:

$$BA \begin{bmatrix} \mathbf{V} \\ -\dot{\boldsymbol{\theta}} \end{bmatrix} = T\dot{\mathbf{Y}}, \quad (23)$$

where B is a selection matrix defined as:

$$\mathbf{B} := \text{diag}(b_1 \mathbf{I}_3, \dots, b_M \mathbf{I}_3) \in \mathfrak{R}^{3M \times 3M}; \quad (24)$$

$$b_l = \begin{cases} 1 & \text{when } P_l \text{ is in virtual sliding,} \\ 0 & \text{otherwise.} \end{cases} \quad (25)$$

We consider all the combinations of b_l except for a trivial case where $\mathbf{B} = \mathbf{O}$; that is, there are $(2^M - 1)$ combinations. A virtual sliding is valid when (23) is satisfied at least for one combination of b_l ; in other words, $\dot{\mathbf{Y}}$ is valid when there exist \mathbf{V} , $\dot{\boldsymbol{\theta}}$ and \mathbf{B} that satisfy (23).

Then, static friction forces can be generated only in the directions to prevent such valid virtual slidings. When P_l is not selected by \mathbf{B} (i.e., $b_l = 0$), no friction forces are generated at P_l as for the corresponding virtual sliding. As a result, a set of valid static friction forces can be calculated for each combination of b_l . The union of each set is the total set of valid static friction forces.

Using this new formulation, the unreasonable results shown in Section III-B can be excluded. The static friction forces shown in Fig. 3(b) are valid in our new formulation because the corresponding virtual object motion (vertically

downward) satisfies (23) when $b_1 = 1$, $b_2 = 1$ and $b_3 = 0$. Similarly, the static friction forces shown in Fig. 5(b) are also valid in our new formulation because the corresponding virtual object motion (horizontally to the right) satisfies (23) when $b_1 = 1$, $b_2 = 1$ and $b_3 = 0$.

B. Calculating Possible Contact Forces Based on New Formulation

Let us investigate the mechanics of the system for a specific selection matrix, \mathbf{B} . As stated above, friction forces cannot exist at the contact points that are not selected by \mathbf{B} . This constraint can be written as follows:

$$\mathbf{T}^T(\mathbf{I}_{3M} - \mathbf{B})\mathbf{f} = \mathbf{0}. \quad (26)$$

The constraint on static friction, which can be derived from that on virtual sliding (23), is very complex. Therefore we adopt a divide-and-conquer approach focusing on the possible signs of the elements of $\dot{\mathbf{Y}}$, as Omata did in [2].

We introduce the following matrix:

$$\mathbf{S} := \text{diag}(s_{11}, s_{12}, \dots, s_{M1}, s_{M2}) \in \mathfrak{R}^{2M \times 2M}, \quad (27)$$

where

$$s_{lm} := \begin{cases} +1 & \text{when } b_l = 1 \text{ and } \dot{Y}_{lm} > 0, \\ -1 & \text{when } b_l = 1 \text{ and } \dot{Y}_{lm} < 0, \\ 0 & \text{when } b_l = 0. \end{cases} \quad (28)$$

There are 2^{2n} patterns for \mathbf{S} at most when \mathbf{B} selects n virtual sliding points. Then we have:

$$\dot{\mathbf{Y}} = \mathbf{S}\mathbf{q}, \quad (29)$$

where $\mathbf{q}(\in \mathfrak{R}^{2M}) > \mathbf{0}$.

The existence of \mathbf{q} that satisfies (23) and (29) for a subcase specified by \mathbf{S} can be tested by solving the following linear programming problem:

$$\begin{aligned} & \underset{\mathbf{q}, \mathbf{V}, \dot{\theta}}{\text{maximize}} \quad \mathbf{1}^T \mathbf{q} \\ & \text{subject to} \quad \begin{cases} \mathbf{B}\mathbf{A} \begin{bmatrix} \mathbf{V} \\ -\dot{\theta} \end{bmatrix} = \mathbf{T}\mathbf{S}\mathbf{q} \\ \mathbf{q} \geq \mathbf{1}, \end{cases} \end{aligned} \quad (30)$$

where $\mathbf{1} = [1, \dots, 1]^T \in \mathfrak{R}^{2M}$. When the objective function diverges to infinity, there exist $\mathbf{q}(> \mathbf{0})$ that satisfies (23) and (29). In that case, the constraint on static friction forces can be written in the following linear form:

$$\mathbf{S}\mathbf{T}^T \mathbf{f} \leq \mathbf{0}. \quad (31)$$

Inequality (31) means that static friction forces can be applied only in the opposite directions of virtual sliding.

From (6), (14), (26) and (31), we can obtain a set of possible contact forces for a subcase specified by \mathbf{S} by solving the following equations and inequalities:

$$\begin{cases} \mathbf{A}^T \mathbf{C}\mathbf{k} = \mathbf{w} \\ \mathbf{T}^T(\mathbf{I}_{3M} - \mathbf{B})\mathbf{C}\mathbf{k} = \mathbf{0} \\ \mathbf{S}\mathbf{T}^T \mathbf{C}\mathbf{k} \leq \mathbf{0} \\ \mathbf{k} \geq \mathbf{0}. \end{cases} \quad (32)$$

The set of possible \mathbf{k} forms a convex hyperpolyhedron in rM -dimensional space for a subcase specified by \mathbf{B} and \mathbf{S} . The corresponding set of possible contact forces, $\mathbf{f} = \mathbf{C}\mathbf{k}$, also forms a convex hyperpolyhedron in $3M$ -dimensional space. The union of each hyperpolyhedron for all the combinations of \mathbf{B} and \mathbf{S} is the total set of possible contact forces, which is not necessarily convex.

Now we can present a complete procedure for the calculation of the total set of possible contact forces as follows:

Step 1. Enumerate all the combinations of virtual sliding/non-sliding contact points (namely, enumerate selection matrices \mathbf{B}).

Step 2. Enumerate all the possible \mathbf{S} for each \mathbf{B} by solving the problem (30).

Step 3. For each combination of \mathbf{B} and \mathbf{S} , solve the problem (32).

Step 4. Obtain the total set of possible contact forces as the union of the results of Step 3.

Under our new formulation, the above procedure enables us to obtain more accurate results on the set of possible indeterminate contact forces than previous studies [1] [2].

V. REDUCTION OF COMPUTATION

If we implement the above procedure straightforwardly, problem (32) must be solved $5^M - 1$ ($= \sum_{n=1}^M \binom{M}{n} 2^{2n}$) times at most. The computation can be very time-consuming when M is large. Thus we investigate the way to reduce the computation.

A. Skipping Impossible Virtual Slidings

Some of $5^M - 1$ patterns can be skipped by considering a property of problem (30). The problem (30) for a combination of \mathbf{B} and \mathbf{S} is sometimes a relaxation problem for other combinations. Therefore in such cases, if a combination of \mathbf{B} and \mathbf{S} is found impossible, we can omit some other combinations immediately. This technique was used also in [3] and [4].

B. Skipping Unnecessary Virtual Slidings

Let us consider a case where a fingertip link of a robot finger has only one contact point. Without loss of generality, we assume that this contact point is $P_M (= P_{NM_N})$. We denote the column vectors of \mathbf{J}_{NM_N} by:

$$\mathbf{J}_{NM_N} = [\mathbf{j}_{NM_N1} \quad \dots \quad \mathbf{j}_{NM_NL_N-1} \quad \mathbf{j}_{NM_NL_N}] \in \mathfrak{R}^{3 \times L_N}, \quad (33)$$

and define the following matrix:

$$\mathbf{Z} := [\mathbf{T}_M \quad \mathbf{j}_{NM_NL_N}] \in \mathfrak{R}^{3 \times 3}. \quad (34)$$

We also use the following notation:

$$\begin{aligned} \mathbf{W} &= [\mathbf{W}_1 \quad \dots \quad \mathbf{W}_{M-1} \quad \mathbf{W}_M] = [\mathbf{W}_- \quad \mathbf{W}_M] \\ \mathbf{W}_i &= \begin{bmatrix} \mathbf{I}_3 \\ \mathbf{p}_i \times \mathbf{I}_3 \end{bmatrix} \in \mathbb{R}^{6 \times 3} \\ \mathbf{J} &= \begin{bmatrix} \mathbf{J}_- \\ \mathbf{J}_* \end{bmatrix} \in \mathbb{R}^{3M \times L} \\ \mathbf{J}_- &\in \mathbb{R}^{3(M-1) \times L} \\ \mathbf{J}_* &= [\mathbf{O} \quad \mathbf{J}_{NM_N}] \in \mathbb{R}^{3 \times L} \\ \mathbf{T} &= \text{diag}(\mathbf{T}_1, \dots, \mathbf{T}_{M-1}, \mathbf{T}_M) = \text{diag}(\mathbf{T}_-, \mathbf{T}_M) \\ \dot{\mathbf{Y}} &= [\dot{\mathbf{Y}}_1^T, \dots, \dot{\mathbf{Y}}_{M-1}^T, \dot{\mathbf{Y}}_M^T]^T = [\dot{\mathbf{Y}}_-^T, \dot{\mathbf{Y}}_M^T]^T. \end{aligned}$$

The selection matrix \mathbf{B} when $b_M = 1$ is given by:

$$\mathbf{B} = \text{diag}(\mathbf{B}_-, \mathbf{I}_3).$$

In this case, (23) can be rewritten as follows:

$$\begin{bmatrix} \mathbf{B}_- & \mathbf{O} \\ \mathbf{O} & \mathbf{I}_3 \end{bmatrix} \begin{bmatrix} \mathbf{W}_-^T & \mathbf{J}_- \\ \mathbf{W}_M^T & \mathbf{J}_* \end{bmatrix} \begin{bmatrix} \mathbf{V} \\ -\dot{\boldsymbol{\theta}} \end{bmatrix} = \begin{bmatrix} \mathbf{T}_- & \mathbf{O} \\ \mathbf{O} & \mathbf{T}_M \end{bmatrix} \begin{bmatrix} \dot{\mathbf{Y}}_- \\ \dot{\mathbf{Y}}_M \end{bmatrix} \quad (35)$$

Similarly, selection matrix \mathbf{B} when $b_M = 0$ is given by:

$$\mathbf{B} = \text{diag}(\mathbf{B}_-, \mathbf{O}_3),$$

where \mathbf{O}_n is the $n \times n$ zero matrix. In this case, (23) can be rewritten as follows:

$$\begin{aligned} \begin{bmatrix} \mathbf{B}_- & \mathbf{O} \\ \mathbf{O} & \mathbf{O}_3 \end{bmatrix} \begin{bmatrix} \mathbf{W}_-^T & \mathbf{J}_- \\ \mathbf{W}_M^T & \mathbf{J}_* \end{bmatrix} \begin{bmatrix} \mathbf{V} \\ -\dot{\boldsymbol{\theta}} \end{bmatrix} &= \begin{bmatrix} \mathbf{T}_- & \mathbf{O} \\ \mathbf{O} & \mathbf{T}_M \end{bmatrix} \begin{bmatrix} \dot{\mathbf{Y}}_- \\ \dot{\mathbf{Y}}_M \end{bmatrix} \\ \therefore \mathbf{B}_- \begin{bmatrix} \mathbf{W}_-^T & \mathbf{J}_- \end{bmatrix} \begin{bmatrix} \mathbf{V} \\ -\dot{\boldsymbol{\theta}} \end{bmatrix} &= \mathbf{T}_- \dot{\mathbf{Y}}_-. \end{aligned} \quad (36)$$

Now we have the following theorem.

Theorem 1: If \mathbf{Z} is nonsingular, for any $\dot{\mathbf{Y}}_-$ that satisfies (36), there exist $\dot{\mathbf{Y}} = [\dot{\mathbf{Y}}_-^T, \dot{\mathbf{Y}}_M^T]^T$ that satisfies (35).

Proof: Equation (35) can be transformed as follows:

$$\begin{aligned} \begin{cases} \mathbf{B}_- \begin{bmatrix} \mathbf{W}_-^T & \mathbf{J}_- \end{bmatrix} \begin{bmatrix} \mathbf{V} \\ -\dot{\boldsymbol{\theta}} \end{bmatrix} = \mathbf{T}_- \dot{\mathbf{Y}}_- \\ \begin{bmatrix} \mathbf{W}_M^T & \mathbf{J}_* \end{bmatrix} \begin{bmatrix} \mathbf{V} \\ -\dot{\boldsymbol{\theta}} \end{bmatrix} = \mathbf{T}_M \dot{\mathbf{Y}}_M \end{cases} & \quad (37a) \\ \therefore \begin{cases} \mathbf{B}_- \begin{bmatrix} \mathbf{W}_-^T & \mathbf{J}_- \end{bmatrix} \begin{bmatrix} \mathbf{V} \\ -\dot{\boldsymbol{\theta}} \end{bmatrix} = \mathbf{T}_- \dot{\mathbf{Y}}_- \\ \begin{bmatrix} \mathbf{W}_M^T & \mathbf{J}_{NM_N} \end{bmatrix} \begin{bmatrix} \mathbf{V} \\ -\dot{\boldsymbol{\theta}} \end{bmatrix} = \mathbf{T}_M \dot{\mathbf{Y}}_M. \end{cases} & \quad (37b) \end{aligned}$$

As shown above, (37a) and (36) are identical equations.

Because of the assumption that the fingertip link of the N -th finger has only one point contact, $\dot{\theta}_{NL_N}$ does not affect the positions of contact points except for P_{NM_N} . Accordingly, $\dot{\theta}_{NL_N}$ does not appear in (36) (and of course, in (37a)); that is, the solution of (36) is specified by $(\mathbf{V}, \dot{\boldsymbol{\theta}}_1, \dots, \dot{\boldsymbol{\theta}}_{N-1}, \dot{\boldsymbol{\theta}}_{N-}, \dot{\mathbf{Y}}_-)$, where $\dot{\boldsymbol{\theta}}_{N-} := [\dot{\theta}_{N1}, \dots, \dot{\theta}_{NL_{N-1}}]^T$.

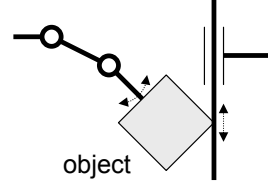


Fig. 6. Examples where \mathbf{Z} is singular

From (37b), we have:

$$\begin{aligned} \begin{bmatrix} \mathbf{W}_M^T & \mathbf{J}_{NM_N} \end{bmatrix} \begin{bmatrix} \mathbf{V} \\ -\dot{\boldsymbol{\theta}}_{N-} \\ -\dot{\theta}_{NL_N} \end{bmatrix} &= \mathbf{T}_M \dot{\mathbf{Y}}_M. \\ \therefore \begin{bmatrix} \mathbf{T}_M & \mathbf{j}_{NM_N LN} \end{bmatrix} \begin{bmatrix} \dot{\mathbf{Y}}_M \\ \dot{\theta}_{NL_N} \end{bmatrix} & \\ = \begin{bmatrix} \mathbf{W}_M^T & \mathbf{j}_{NM_N 1} & \dots & \mathbf{j}_{NM_N LN-1} \end{bmatrix} \begin{bmatrix} \mathbf{V} \\ -\dot{\boldsymbol{\theta}}_{N-} \end{bmatrix} & \\ \therefore \mathbf{Z} \begin{bmatrix} \dot{\mathbf{Y}}_M \\ \dot{\theta}_{NL_N} \end{bmatrix} = & \\ \begin{bmatrix} \mathbf{W}_M^T & \mathbf{j}_{NM_N 1} & \dots & \mathbf{j}_{NM_N LN-1} \end{bmatrix} \begin{bmatrix} \mathbf{V} \\ -\dot{\boldsymbol{\theta}}_{N-} \end{bmatrix}. & \end{aligned}$$

Therefore, if \mathbf{Z} is nonsingular, we can find $\dot{\mathbf{Y}}_M$ and $\dot{\theta}_{NL_N}$ that satisfy (37b) for solution of (36). That is, for any $\dot{\mathbf{Y}}_-$ that satisfies (36), there exist $\dot{\mathbf{Y}} = [\dot{\mathbf{Y}}_-^T, \dot{\mathbf{Y}}_M^T]^T$ that satisfies (35). ■

Theorem 1 enables us to skip combinations of \mathbf{B} whose $b_M = 0$ in the calculation of possible contact forces when \mathbf{Z} is nonsingular. In other words, nonsingularity of \mathbf{Z} is a sufficient condition to skip some unnecessary virtual slidings.

We can reduce the computation when this sufficient condition holds. For example, if each of fingertip links of all the fingers has only one contact point and \mathbf{Z} is nonsingular for each, the number of the combinations of \mathbf{B} to be considered is reduced from $(2^M - 1)$ to 2^{M-N} . \mathbf{Z} is singular only in special cases as shown in Fig. 6.

VI. NUMERICAL EXAMPLES

We implemented the procedure presented in Section IV-B for calculating the set of possible indeterminate contact forces as a program on Linux. The program uses cdd [7] for solving (30) and (32).

Because of the page limitation, we present a few simple numerical examples. The computation times for the examples are measured on a PC with Pentium4–3.2GHz. The friction coefficient is set to 0.5 in all the contact points.

A. Example: Planar Grasp

Let us consider the case of Fig. 3. The parameters are as follows:

$$\begin{aligned} \mathbf{w}_{\text{ext}} &= [0, -1, 0]^T, \quad \boldsymbol{\tau} = [1, -1]^T \\ \mathbf{p}_1 &= \begin{bmatrix} -0.1 \\ 0 \end{bmatrix}, \quad \mathbf{p}_2 = \begin{bmatrix} 0.1 \\ 0 \end{bmatrix}, \quad \mathbf{p}_3 = \begin{bmatrix} 0 \\ 0.1 \end{bmatrix} \end{aligned}$$

$$\mathbf{J} = \begin{bmatrix} 0.1 & 0 & 0 \\ 0 & 0 & 0 \\ 0 & 0.1 & 0 \\ 0 & 0 & 0 \\ 0 & 0 & 0 \\ 0 & 0 & 0 \end{bmatrix}, \quad \mathbf{T} = \begin{bmatrix} 0 & 0 & 0 \\ -1 & 0 & 0 \\ 0 & 0 & 0 \\ 0 & 1 & 0 \\ 0 & 0 & -1 \\ 0 & 0 & 0 \end{bmatrix}.$$

In this case, Theorem 1 can be applied to P_1 and P_2 , and \mathbf{Z} is nonsingular in both cases. Therefore, we should consider only the following two patterns for \mathbf{B} :

$$\mathbf{B} = \text{diag}(\mathbf{I}_2, \mathbf{I}_2, \mathbf{I}_2), \quad \text{diag}(\mathbf{I}_2, \mathbf{I}_2, \mathbf{O}_2).$$

In fact, the possible contact forces that satisfy (23), (29) and (32) can be calculated only when $\mathbf{B} = \text{diag}(\mathbf{I}_2, \mathbf{I}_2, \mathbf{O}_2)$ and $\mathbf{S} = \text{diag}(1, -1, 0)$. The total set of possible indeterminate contact forces, \mathcal{F} , is as follows:

$$\mathcal{F} = \{\mathbf{f} \mid \mathbf{f} = k_A \mathbf{f}_A + k_B \mathbf{f}_B, k_A + k_B = 1, k_{A,B} \geq 0\},$$

where

$$\mathbf{f}_A = [10, 0.5, -10, 0.5, 0, 0]^T \\ \mathbf{f}_B = [10, 5, -10, 5, 0, -9]^T.$$

This grasp is hyperstatic [8]. The computation time for this case is 0.004 and 0.007 seconds with and without Theorem 1, respectively.

B. Example: Non-grasped Object

The next example is the case of Fig. 5. In this case, we do not have to consider \mathbf{J} and $\boldsymbol{\tau}$ because there are no robot joints, and Theorem 1 is not applicable. The parameters are as follows:

$$\mathbf{w}_{\text{ext}} = [0.2, -1, 0]^T \\ \mathbf{p}_1 = \begin{bmatrix} -0.1 \\ -0.1 \end{bmatrix}, \quad \mathbf{p}_2 = \begin{bmatrix} 0.1 \\ -0.1 \end{bmatrix}, \quad \mathbf{p}_3 = \begin{bmatrix} -0.1 \\ 0 \end{bmatrix} \\ \mathbf{T} = \begin{bmatrix} 1 & 0 & 0 \\ 0 & 0 & 0 \\ 0 & 1 & 0 \\ 0 & 0 & 0 \\ 0 & 0 & 0 \\ 0 & 0 & -1 \end{bmatrix}.$$

In this case, the possible contact forces that satisfy (23), (29) and (32) can be calculated in the following subcases:

$$\mathbf{B} = \text{diag}(\mathbf{I}_2, \mathbf{O}_2, \mathbf{O}_2), \quad \mathbf{S} = \text{diag}(1, 0, 0) \\ \mathbf{B} = \text{diag}(\mathbf{O}_2, \mathbf{I}_2, \mathbf{O}_2), \quad \mathbf{S} = \text{diag}(0, 1, 0) \\ \mathbf{B} = \text{diag}(\mathbf{I}_2, \mathbf{I}_2, \mathbf{O}_2), \quad \mathbf{S} = \text{diag}(1, 1, 0) \\ \mathbf{B} = \text{diag}(\mathbf{O}_2, \mathbf{I}_2, \mathbf{I}_2), \quad \mathbf{S} = \text{diag}(0, 1, 1).$$

The total set of possible indeterminate contact forces, \mathcal{F} , is expressed by eliminating overlap as follows:

$$\mathcal{F} = \mathcal{F}_1 \cup \mathcal{F}_2 \\ \mathcal{F}_1 = \left\{ \mathbf{f} \mid \mathbf{f} = \sum_{i=1}^3 k_{Bi} \mathbf{f}_{Bi}, \sum_{i=1}^3 k_{Bi} = 1, k_{Bi} \geq 0 \right\} \\ \mathcal{F}_2 = \left\{ \mathbf{f} \mid \mathbf{f} = \sum_{i=1,2,4} k_{Bi} \mathbf{f}_{Bi}, \sum_{i=1,2,4} k_{Bi} = 1, k_{Bi} \geq 0 \right\} \\ \mathbf{f}_{B1} = [0, 0.4, -0.2, 0.6, 0, 0]^T \\ \mathbf{f}_{B2} = [0, 0.333, -0.333, 0.667, 0.133, 0]^T \\ \mathbf{f}_{B3} = [-0.2, 0.4, 0, 0.6, 0, 0]^T \\ \mathbf{f}_{B4} = [0, 0.267, -0.333, 0.667, 0.133, 0.067]^T.$$

The computation time for this case is 0.007 seconds.

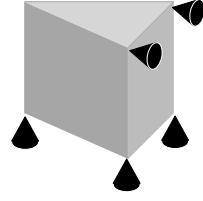


Fig. 7. A triangular prism supported by five contacts

C. Example: A Spatial Case

Our method was successfully applied to spatial cases. As an example, let us introduce a case of a triangular prism supported by five contact points as shown in Fig. 7. In this case, the total set of possible contact forces was calculated as a union of 80 convex hyperpolyhedra. The computation time was 9.1 seconds when $r = 48$.

VII. CONCLUSION

In this paper, we investigated the indeterminate contact forces in robotic grasping and contact tasks. We showed that Omata and Nagata's formulation [1] [2], which was originally derived for power grasps, sometimes generates unreasonable results on possible contact forces. Then we presented a modified version of their formulation that can exclude such unreasonable results. We also derived a sufficient condition to reduce the computation of possible indeterminate contact forces in our new formulation.

In future work, we will pursue more efficient computation in the new formulation. The proposed framework should be applied to various problems of robotic grasping as well as those of robotic contact tasks [3] [4].

ACKNOWLEDGMENTS

This work was partly supported by Japanese Ministry of Education, Culture, Sports, Science and Technology, Grant-in-Aid for Young Scientists (B), No. 18700197.

REFERENCES

- [1] T. Omata and K. Nagata, "Rigid body analysis of the indeterminate grasp force in power grasps," *IEEE Trans. on Robotics and Automation*, vol. 16, no. 1, pp. 46–54, 2000.
- [2] T. Omata, "Rigid body analysis of power grasps: Bounds of the indeterminate grasp force," in *Proc. of IEEE Int. Conf. on Robotics and Automation*, Seoul, Korea, 2001, pp. 2203–2209.
- [3] Y. Maeda, "On the possibility of excessive internal forces on manipulated objects in robotic contact tasks," in *Proc. of IEEE Int. Conf. on Robotics and Automation*, Barcelona, Spain, 2005, pp. 1953–1958.
- [4] Y. Maeda and S. Makita, "A quantitative test for the robustness of graspless manipulation," in *Proc. of IEEE Int. Conf. on Robotics and Automation*, Orlando, FL, U.S.A., 2006, pp. 1743–1748.
- [5] Y. Aiyama, M. Inaba, and H. Inoue, "Pivoting: A new method of graspless manipulation of object by robot fingers," in *Proc. of IEEE/RSJ Int. Conf. on Intelligent Robots and Systems*, Yokohama, Japan, 1993, pp. 136–143.
- [6] S. Hirai and H. Asada, "Kinematics and statics of manipulation using the theory of polyhedral convex cones," *Int. J. of Robotics Research*, vol. 12, no. 5, pp. 434–447, 1993.
- [7] K. Fukuda, "cdd," http://www.ifor.math.ethz.ch/~fukuda/cdd_home/.
- [8] D. Prattichizzo and A. Bicchi, "Dynamic analysis of mobility and graspability of general manipulation systems," *IEEE Trans. on Robotics and Automation*, vol. 14, no. 2, pp. 241–258, 1998.